symmetry

MDPI

Article

Automobile Driver Fatigue Detection Method Based on Facial Image Recognition under Single Sample Condition

Cangyan Xiao [1], Liu Han [2,*] and Shuzhao Chen [2]

[1] School of Transportation Engineering, Jiangsu Vocational Institute of Architectural Technology, Xuzhou 221116, China; 10859@jsjzi.edu.cn
[2] School of Mines, China University of Mining and Technology, Xuzhou 221116, China; 5155@cumt.edu.cn
* Correspondence: 5757@cumt.edu.cn

Abstract: Under the existing single sample condition, the fatigue detection method of an automobile driver has some problems, such as an improper camera calibration method, image denoising beyond the controllable range, low fatigue detection accuracy, and unsatisfactory effect. A fatigue detection method for drivers based on face recognition under a single sample condition is proposed. Firstly, the camera is calibrated by Zhang Zhengyou's calibration method. The optimal camera parameters were calculated by linear simulation analysis, and the image was nonlinear refined by the maximum likelihood method. Then, the corrected image effect is enhanced, and the scale parameter gap in the MSRCR image enhancement method is adjusted to the minimum. The detection efficiency is improved by a symmetric algorithm. Finally, the texture mapping technology is used to enhance the authenticity of the enhanced image, and the face image recognition is carried out. The constraint conditions of fatigue detection are established, and the fatigue detection of car drivers under the condition of a single sample is completed. Experimental results show that the proposed method has a good overall detection effect: the fatigue detection accuracy is 20% higher than that of the traditional method, and the average detection time is over 30%. Compared with the traditional fatigue detection methods, this method has obvious advantages, can effectively extract more useful information from the image, and has strong applicability.

Keywords: facial image; single sample; automobile driver; fatigue detection

Citation: Xiao, C.; Han, L.; Chen, S. Automobile Driver Fatigue Detection Method Based on Facial Image Recognition under Single Sample Condition. *Symmetry* **2021**, *13*, 1195. https://doi.org/10.3390/sym13071195

Academic Editor: Juan Luis García Guirao

Received: 23 March 2021
Accepted: 21 June 2021
Published: 2 July 2021

1. Introduction

The automobile is an indispensable mechanical equipment in the agricultural production and life. The driving technology and driving state of the automobile driver will have a direct impact on the quality of agricultural cultivation. Agricultural production is seasonally strong, working hours are concentrated, and the working environment is relatively bad, so automobile drivers are prone to fatigue [1]. However, in real life, people often ignore the fatigue analysis of the automobile driver, so it is of great practical significance to strengthen the fatigue analysis of the automobile driver to ensure the effective production of agricultural production. At present, there are many methods to detect faces. When a sufficient number of representative samples are detected, good results can be obtained. However, in some specific cases, only one automobile driver's face image is used for detection. When dealing with this single sample detection problem, the detection efficiency of the existing research methods will appear to be significantly reduced [2,3]. In order to better describe the face state of automobile drivers, it is necessary to detect the fatigue of automobile drivers under the condition of a single sample [4,5]. The common methods are Maya, XSI, and monocular and binocular vision, but in terms of image resolution, it cannot meet the needs of detection, resulting in an unsatisfactory detection result [6]. In contrast, the automobile driver's fatigue detection is realistic under the single sample condition established by the facial image recognition technology, and the texture details

of the original driver's face are preserved, which is a reliable detection method. Several fatigue testing methods are introduced.

In reference [7], a deep hybrid neural network model is proposed to recognize the driver's eye opening and closing state. The model combines two models of deep neural network and deep convolution neural network and constructs a joint cost function according to the output of each model. The optimal model is obtained by optimizing the joint cost function to recognize the open and closed state of eyes. However, the monitoring effect of this method is poor. A new driver fatigue detection method is proposed in reference [8]. The infrared image acquisition system adopts the method of combining AdaBoost and kernel correlation filtering to collect the driver's face image and subsequently detect and track the face. The cascade regression method is used to locate feature points and extract eye and mouth regions. Convolution neural network is used to recognize the state of the eyes and mouth. However, the monitoring accuracy of this method is low. In reference [9], a new face recognition algorithm based on a single sample is proposed. The algorithm can not only keep the relationship between the original data in low-dimensional space but also improve the accuracy of face recognition. Experiments on AR, yale-b, and the extended yale-b face database demonstrate the effectiveness of the proposed face change model framework and its algorithm. However, it is complex to solve the transform matrix of discontinuous moving frames, the fatigue detection error is large, and the texture details of face detection results are not good enough.

Aiming at the above problems, an automobile driver fatigue detection method based on facial image recognition is proposed under a single sample condition. The overall arrangement of the article is as follows:

(1) First, we use the calibration method of Zhang Zhengyou to calibrate the automobile driver's face image under the influence of lens distortion.
(2) The scale parameter gap in the MSRCR image enhancement method is adjusted to the minimum, the image histogram is combined to make the image suitable for human eye vision, and the automobile driver's face is enhanced.
(3) Firstly, texture mapping technology is used to strengthen the authenticity of the enhanced image, facial image recognition is processed, and the constraints of fatigue detection are established to complete the automobile driver fatigue detection.
(4) Experimental results and analysis verify the validity of the detection method.
(5) Discussion.
(6) To summarize the contents of the full text and look forward to the future.

2. Materials and Methods

The camera calibration is very important for the automobile driver fatigue detection under a single sample condition, and the camera calibration is realized by using the calibration method of Zhang Zhengyou.

2.1. Camera Calibration of Automobile Driver Fatigue Detection

In the calibration method of Zhang Zhengyou, it is assumed that the plane calibration board is used in the coordinate system, the optimal solution of the camera parameters is calculated by linear simulation analysis, the maximum likelihood method is used for nonlinear refinement, and the effect of lens distortion is taken into account in the calibration. The specific methods are as follows.

The calculation of the homography matrix: a mapping between the point of the template plane and its image points is called the homography matrix H. Suppose that:

$$H = \begin{bmatrix} h_{11} & h_{12} & h_{13} \\ h_{21} & h_{22} & h_{23} \\ h_{31} & h_{32} & 1 \end{bmatrix}. \quad (1)$$

The elements in the matrix are:

$$h = \begin{bmatrix} x_w & y_w & 1 & 0 & 0 & 0 & u\,x_w \\ 0 & 0 & 0 & x_w & y_w & 1 & vx_w \end{bmatrix}. \tag{2}$$

Among them, u is the proportional coefficient, v is the weight parameter, x_w represents the abscissa, and y_w represents the ordinate.

Let $H = [h_1 \;\; h_2 \;\; h_3]$. Then:

$$[h_1 \;\; h_2 \;\; h_3] = \lambda A[r_1 \;\; r_2 \;] \tag{3}$$

where λ represents the orthogonal factor, and r_1 and r_2 represent the external parameters of the camera; then:

$$\begin{cases} h_1^T A^{-T} A^{-1} h_2 = 0 \\ h_{-1}^T A^{-T} A^{-1} h_1 = h_2^T A^{-T} h_2 \end{cases} \tag{4}$$

where A represents the camera's internal parameters, T represents the transposed symbols, $-T$ is the reverse direction transposition, and -1 is the first transposition. Formula (4) provides two constraints for the solution of the internal parameters of the camera, with the 6 degrees of freedom occupied by the external parameters, which just satisfies all 8 degrees of freedom of the single stress matrix of the plane calibration template.

Then, the camera parameters are solved. Suppose that the symmetric matrix B is:

$$B = A^{-T}A^{-1} = \begin{bmatrix} B_{11} & B_{12} & B_{13} \\ B_{21} & B_{22} & B_{23} \\ B_{31} & B_{32} & B_{33} \end{bmatrix} = \begin{bmatrix} \frac{1}{x_w^2} & \frac{sv-uf_y}{x_w^2 y_w} & -\frac{s}{x_w^2 y_w^2} \\ -\frac{s}{x_w^2 y_w^2} & \frac{s}{x_w^2 y_w} + \frac{1}{y_w} & -\frac{s(sv-uy_w)}{x_w^2 y_w^2} - \frac{v}{y_w^2} \\ \frac{sv-uy_w}{x_w^2 y_w} & -\frac{s(sv-uy_w)}{x_w^2 y_w^2} - \frac{v}{y_w^2} & \frac{s(sv-uy_w)}{x_w^2 y_w^2} + \frac{v}{y_w^2} + 1 \end{bmatrix}. \tag{5}$$

In Formula (5), s is the number of degrees of freedom, and the vector b is defined as $b = [B_{11} \;\; B_{12} \;\; B_{22} \;\; B_{13} \;\; B_{23} \;\; B_{33}]^T$, then:

$$h_1^T B h = v^T b. \tag{6}$$

According to the constraint condition of Formula (4), we can get the homogeneous equation vector b:

$$\begin{bmatrix} v_{12}^T \\ (v_{11} - v_{22})^T \end{bmatrix} b = 0. \tag{7}$$

On the basis of Formula (7), a set of linear equations can be obtained:

$$V = \begin{bmatrix} h_{11} & h_{12} & \dots & h_{1r} \\ h_{21} & h_{22} & \dots & h_{2r} \\ \vdots & \vdots & & \vdots \\ h_{r1} & h_{r2} & \dots & h_{rr} \end{bmatrix}. \tag{8}$$

In Formula (8), V represents a matrix of $2n \times 6$. Assuming that the data of the template image is $n \geq 3$, 6 equations can be listed, and b is solved. Matrix B can be obtained by obtaining b, and the key parameters of each direction of the camera can be obtained by Formula (5).

$$\begin{cases} c_y = (B_{12}B_{13} - B_{11}B_{23}) / \left(B_{11}B_{22} - B_{12}^2\right) \\ k = B_{33} - \left[B_{13}^2 + c_y(B_{12}B_{13} - B_{11}B_{23})\right] / B_{11} \\ x_w = \sqrt{k / B_{11}} \\ y_w = \sqrt{kB_{11} / \left(B_{11}B_{22} - B_{12}^2\right)} \\ s = -B_{12}x_w^2 y_w / k \\ c_x = sc_y - B_{13}x_w^2 \end{cases} \tag{9}$$

In Formula (9), c_x, c_y, and k are the camera aperture, wide angle focal length, and pixel, respectively. The camera's external parameters at different viewpoints can be obtained by the following formula:

$$r_1 = \lambda A^{-1} h_1,\ r_2 = \lambda A^{-1} h_2,\ r_3 = r_1 * r_2,\ r_n = \lambda A^{-1} h_3,\ \lambda = 1/\|A^{-1} h_1\| = 1/\|A^{-1} h_2\|. \quad (10)$$

Finally, the maximum likelihood estimation method is used to solve the results accurately. Suppose there are n images on the calibration template; each image has m points, and the data of each point are affected by the noise independently distributed. The objective function is to be set up as follows:

$$\min \sum_{i=1}^{n} \sum_{j=1}^{m} \left\| m_{ij} = c_x \widehat{m}\left(A, R_i, t_i, M_j\right) \right\|^2. \quad (11)$$

In the result of Formula (11), m_{ij} represents the image coordinates of the j point in the i amplitude image, R_i and t_i represent the rotation and translation vectors of the i amplitude image coordinates, M_j represents the obtained image point coordinates, and $\widehat{m}\left(A, R_i, t_i, M_j\right)$ represents the world coordinates of the j point in the i amplitude image. Error characteristic curves were used to evaluate the positioning accuracy of the proposed method in different datasets, with the formula as.

$$s_k^- = V_S - V_{CE}. \quad (12)$$

In the result of Formula (12), V_S represents the error in the coordinates, and V_{CE} represents the total number of test samples.

To sum up, the calibration method of Zhang Zhengyou does not need to refine the calibration block; the calibration process has good robustness, the internal and external parameters of the camera and the distortion coefficient can be all obtained at one time with high precision and strong practicability [10,11].

The double object vision calibration method is used in this paper, and the double target determination experiment is divided into two parts of the automobile driver's face image acquisition and image calibration. The image calibration part is composed of a calibration board and calibration software. As shown in Figure 1, the left and right cameras are fixed in parallel on the bracket to form a binocular camera, and the calibration board is about 1 to 2 m away from the camera. Suppose that the world coordinate system coincides with the left camera coordinate system; the lens focal length is adjusted to make the image sharpness reach the best state and improve the automobile driver's fatigue detection precision under the single sample condition. The calibration board used in the experiment is made by the calibration board template provided by the HALCON machine vision software. HALCON is developed by a German company and is one of the most versatile types of machine vision software today [12]. It provides a variety of libraries with outstanding performance controllers, and users can make use of their open architecture to quickly develop programs in the fields of image processing and machine vision. The calibration board has 8x8 dots, and the center distance is 40mm. The right upper corner of the boundary rectangular frame of the demarcated plate has a mark. It can make the camera calibration method obtain the displacement direction of the calibration board. The circle mark can be used to extract the center coordinates very accurately. The circular marking points are arranged in a rectangular array, which makes the camera calibration method more convenient in regard to extracting the pixels corresponding to the mark points.

According to the characteristics of the calibration board, the $m * n$ circle area inside the calibrated plate can be obtained by the threshold segmentation operation. Once the internal region of the calibrated object is found, the edge of each circle on the calibrated board can be extracted by the sub pixel edge extraction method, and the coordinates of each center can be obtained. The specific calibration process is as follows:

(1) Keep the binocular camera fixed and move the calibration board, and get a number of calibration plate images at different angles.
(2) Detect the center of the face in the facial image.
(3) Solve all internal and external parameters of the camera based on closed solution.
(4) All parameters, including distortion parameters, can be accurately solved based on the minimum solution of Formula (11).

Figure 1. Binocular stereo vision camera.

2.2. Image Enhancement of Automobile Driver's Face

In Section 2.2, the noise is distributed in the target point, and the image of the driver's face is also noisy. This section focuses on the analysis and improvement of the Retinex method in the image enhancement method. On this basis, a special color image enhancement method (MSRCR) suitable for human eye vision is proposed on the basis of an image histogram. When the MSRCR method is applied to the face image enhancement of the automobile driver, in order to obtain the best effect, the gap of the scale parameters is adjusted to the minimum, and the visual characteristics of the human eye are considered. The color, brightness, and contrast of the image are compared with the visual effect of the human eye. The detailed process is as follows:

(1) Global processing of the automobile driver's facial image is done on the logarithmic domain, and the dynamic range of the image is obtained and adjusted preliminarily.
(2) Multi-scale processing to adjust the local dynamic range of the automobile driver's facial images.
(3) Adaptive change of color is realized on the assumption of GreyWorld.
(4) Histogram correction is used to further improve the global contrast of the automobile driver's facial images.

Due to a certain assumption in the algorithm, the partial image obtained through step three is dark and cannot achieve the best visual effect. Therefore, the global contrast of the image is adjusted by the histogram interception in step four [13,14]. In this method, parameters are mainly controlled by hand, which are obtained by experiment, and the choice of parameters has little effect on the quality of image enhancement. By using the histogram information of the image, we can make some improvements to step four.

In the image enhancement method, linear contrast stretching is a simple and effective algorithm, which is as follows:

$$I_{out} = \begin{cases} 0 & if \quad I_{in} \le I_{low} \\ \frac{I_{in} - I_{low}}{I_{hi} d_{\max}} \le I_{low} & if \quad I_{low} < I_{in} < I_{hi} \\ d_{\max} & if \quad I_{in} > I_{hi} \end{cases} . \tag{13}$$

Among them, I_{out} and I_{in} represent the output and input (the image obtained in step 3), I_{low} represents the minimum value to obtain the image, and $d_{\max}$ represents the dynamic range of the display device. Assuming that I_{hi} represents the maximum $I_{\max}$ of the display device, the image enhancement method is a common linear contrast stretching method considering the dynamic range of display devices. Assuming that it is directly applied to step (4) of the MSRCR method without considering the specific content of the image, the enhancement effect is not obvious. Thus, for I_{hi} and I_{low}, from the histogram distribution of images, an adaptive selection intercept point I_{hi} and I_{low} is given.

The probability of each gray value in the image of automobile driver is:

$$P(I_z) = \frac{l_z}{l}. \tag{14}$$

Among them, l_z represents the number of pixels with a gray scale of z, and l represents the total image prime number. $P(I_z)$ represents the value of the image histogram, as shown in Figure 2, where the low-end intercept point and the high-end intercept point are the I_{hi} and I_{low} mentioned above.

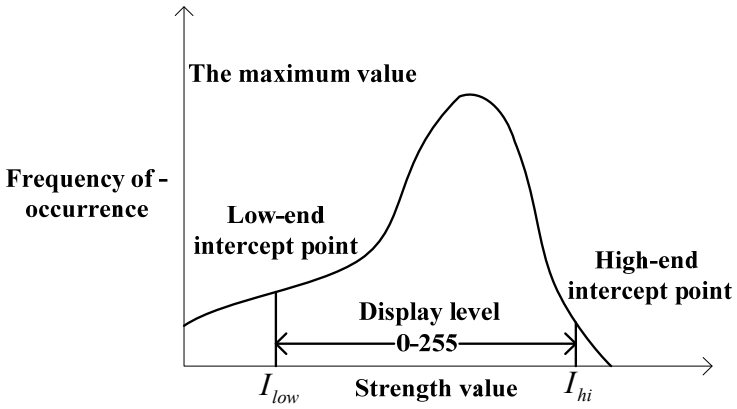

Figure 2. Image histogram.

Suppose that:

$$C_z(I_z) = \sum_{z=1}^{i} P(I_z). \tag{15}$$

Formula (14) is called a cumulative distribution function (CDF), which represents the proportion of pixels of an image under certain intensity. In the contrast enhancement of images, a certain proportion of pixels will reach saturation or lower saturation, which is expressed by I_{hi} and I_{low}, and these two points can be found by analyzing the relationship between the CDF and the histogram. Specifically, using $P(I_{low})$ and $P(I_{hi})$ to represent the probability of upper saturation and lower saturation, the corresponding image intensities are I_{hi} and I_{low}, as shown in Figure 3.

When CDF exceeds a probability of $P(I_{low})$ at a certain gray level, I_{low} is obtained:

$$I_{low} = I_z \; when \; C(I_z) \geq P(I_{low}). \tag{16}$$

Start with $z = 1$ and accumulate until the z and I_z that satisfy the requirement were found. In the same way, I_{hi} can be obtained, that is:

$$I_{hi} = I_z \; when \; [1 - C(I_z)] > P(I_{hi}). \tag{17}$$

At this point, start searching from $z = z_{\max}$ and decrease until you find the z and I_z that satisfy the condition. Thus, the cumulative distribution function can be used to obtain the saturated intercept point adaptively and complete the automobile driver's face image enhancement.

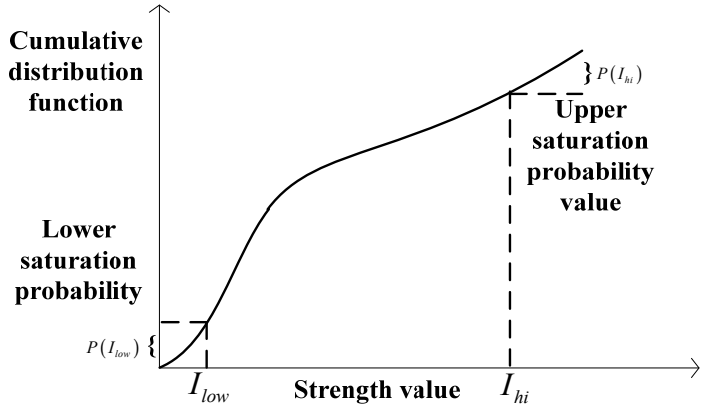

Figure 3. Cumulative distribution function diagram.

In order to further enhance the image, texture mapping is used to map texture images onto spatial entities. The key of this operation is to establish the correspondence between object spatial coordinates and texture spatial coordinates. The image of a complex object can be pasted to a simple geometric body surface by using the texture mapping technology. When displaying the space scene in real time, it can also make use of the translation of the 3D image and rotation to realize the effect of the rotation of the complex object with the change of the observation direction. The texture mapping process is to make texture patterns in a texture space, determine the mapping relationship between points on the surface of the space object and the points in the texture, and map the texture patterns of the texture space to the object according to a certain technique.

There are many kinds of texture picture formats that can be used for textures. Commonly used formats are JPG and RGB format. Since the operation is in ArcGIS and the Windows system, the texture format chosen in this test is BMP format. Mapping only gives us the spatial frame of the face image of our automobile driver. In order to enhance the realistic sense of the automobile driver's face image, it is necessary to assign the texture map to the surface of the automobile to make it more real, which is essential to the map. The quality of the map is very important, which directly affects the visual effect. The image is enhanced by the image enhancement in Section 2.2. The brightness of the texture image is improved, and the texture map is realized in the material editor of the facial image recognition, as shown in Figure 4.

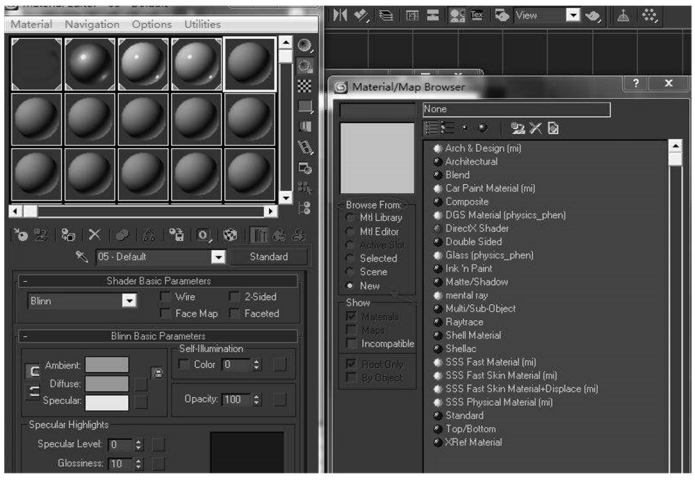

Figure 4. Face identification material editor.

Through the above introduction, we use the "material editor" to simulate the effects of the luster, texture, and shade of the driver's face, so that the performance of the face image

can be more close to the real; at the same time, the texture and the related information under the single sample condition are expressed [15–18]. It is worth noting that it is difficult to make the map match the correct map coordinate and size on the different surfaces of the object, and it must be done well to realize the true simulation effect. Therefore, we need to use the "UVW expansion" map modifier to manage the coordinates of the map. The "UVW" refers to the map coordinate system, which is different from the XYZ spatial coordinate system in the image recognition scene. The coordinates of U, V, and W are parallel to the direction of the X, Y, and Z coordinates. If the space map is viewed, U is equivalent to the direction of the X mapping level, V is equivalent to Y representing the vertical direction of the map, and W is equivalent to the Z representing the vertical direction of the UV plane with the map.

The UVW expansion map modifier expands the UVW coordinates into plane coordinates, so that these surfaces can be expanded into planes, and the relationship between the map and the surface of the object can be visually controlled. The use of a UVW expansion modifier can accurately control texture mapping and map the texture map to the surface of the object accurately, which is especially suitable for the automobile driver fatigue detection under single sample conditions and further enhances the face image of the automobile driver.

2.3. Automobile Driver Fatigue Detection under Single Sample Condition Based on Face Image Recognition

This section first carries out facial image recognition, uses the vertical projection method to determine the comfort value of the face, and establishes the constraints of fatigue detection. Symmetric cryptography has the advantages of high efficiency, simple algorithm, low system overhead, and suitability for encrypting large amounts of data. The automobile driver fatigue detection under a single sample condition is realized [19–21].

The enhanced image background is basically filtered out, leaving only face images and some small non-face areas, and the face area occupies a large part of the whole image [22]. At this point, we can use vertical projection to determine the comfort value $P(x)$ of the face:

$$P(x) = \sum_{x=1}^{N} I(x). \tag{18}$$

In Formula (17), $I(x)$ is a vertical projection function. When the face comfort value $P(x)$ is greater than 0, the automobile driver is in a fatigue state; when $P(x)$ is equal to 0, the automobile driver is in general condition; when the $P(x)$ is less than 0, the automobile driver is in a comfortable state.

The comfort value of the face image is obviously different from the background of other objects, and the comfort distribution value of the face is also different, but it has little effect on the average comfort value of the face, and the rest of the face is relatively uniform, so in the area where the face is located, the projection curve will appear relatively flat, and the face and background will be recognized. There is a sudden change at the boundary; that is, there will be a big gradient at the point of the boundary. In the vertical projection, as long as we find the coordinates with the largest change of gray level, we can determine the comfort value of the human face. The next step we need to do is delete the remaining non-face regions and use connected region markers to further process them. The connected label processing operation of the enhanced image is to extract the pixel set with the pixel value of "1" from the dot matrix image composed of white pixels and black pixels and then fill different digital labels in different connected regions of the image to get the detection value of statistical connected region as

$$V_k = \Sigma_k(R_t, R_o). \tag{19}$$

In the formula, R_t, R_o are the output parameters and partial nodes of the image group diagram, respectively. The face part is a connected domain, and it is a connected domain

with the largest connectivity area in the whole image. The rest of the non-face region is filled with black. Then, we further look for the upper and lower boundaries of the face in the image, which can be done directly from the top down to the first white pixel point. At this point, the face comfort value has been found, and then, the face area can be cut from the original image.

From the cut face area, it is known that the connecting line of any two points on the face of the automobile driver is parallel and equal in the translation, the vector of any position on the driver's face is different, and the difference is a constant vector. Therefore, the driver's face fatigue detection elements under a single sample condition can be divided into three major categories: spot, linear, and surface.

Spot element analysis. The spot elements include the face and mouth organs of the automobile driver. In the facial image recognition technology, the spot of the automobile driver's face is constructed by using the texture mapping method. First, two images under the same single sample condition are prepared, one of which is black and white; a BOX is created, and a phase is added. A spotlight is used as the main light source, and a reflector is used as an auxiliary light. The material editor is used for editing, and then the spotlight is changed to modify the panel.

Analysis of linear elements. Linear elements include the automobile drivers' facial lines, connections, and so on. First, the line is extended in the facial image recognition technology, and then, the subsequent texture map is made.

Analysis of surface elements. The surface elements include large areas except for eyes, eyebrows, lines, etc. In facial image recognition technology, because the main object of the detection model is a regular set of faces, it is usually analyzed by polygons. The analysis method can be summed up by the following two points:

(1) Through the analysis of the face appearance of the automobile driver under a single sample condition, the main body under a single sample condition is constructed as much as possible by using as little simple aggregate as possible.
(2) Omitting local details, highlighting the local appearance with characteristic marks, making use of editable lines for outline drawing, drawing lines into faces, and extruding molding.

After two steps of space construction and texture mapping, the automobile driver's face fatigue detection under a single sample condition is basically completed, and then, the image is output. In order to apply the detection method under the single sample condition in the ARCGIS software, it is necessary to carry out the matching material in the output of the test result and put the map in the same directory with the map; otherwise, the texturing effect of the material will not be displayed in the ARCGIS.

To sum up, the fatigue test of automobile drivers under a single sample condition is completed.

3. Results

In order to verify the overall effectiveness of the method, the relevant experiments are carried out through the sample dataset. The Argoverse dataset is a dataset published by Argo AI, Carnegie Mellon University and Georgia Institute of Technology to support 3D Tracking and Motion Forecasting autopilotresearch. The dataset consists of two parts: argover 3D tracking and argover motion forecasting.

The Argoverse dataset contains lidar data, RGB video data, forward binocular data, 6 DOF positioning data, and high-precision map data. All the data are registered with high-precision map data.

Argoverse is the first dataset containing a high-precision map, which contains 290 km high-precision map data with geometric shapes and semantic information.

Analysis of Figures 5 and 6 showed that the automobile driver's image enhancement effect and camera calibration results obtained by the proposed method are ideal. The calibration method of Zhang Zhengyou calculates the optimal solution of the camera parameters by linear simulation analysis; then, the maximum likelihood method was used

for nonlinear refinement, and the effect of lens distortion was taken into account in the calibration, which makes the calibration result more reasonable. MSRCR considered the visual characteristics of the human eye; the color, brightness, and contrast of the image are compared with the visual effect of the human eye, and the histogram modification is used to further improve the global contrast of the image and the image enhancement effect.

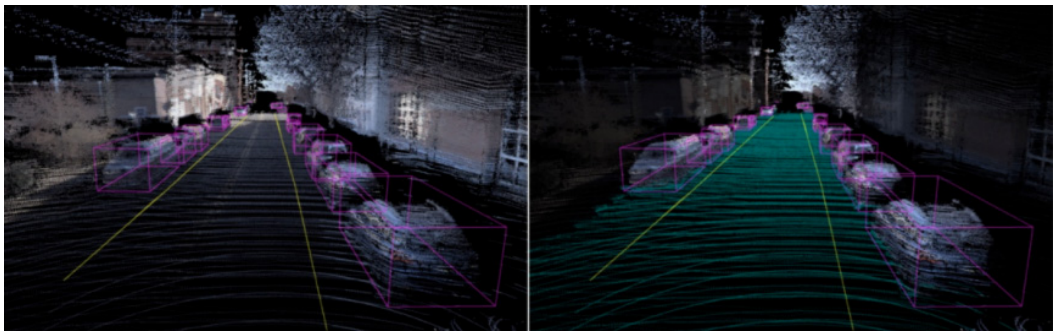

Figure 5. 3D visualization of an Argoverse scene.

(**A**)Unenhanced automobile driver's face image.

(**B**)Automobile driver face image enhanced by current method.

(**C**) Automobile driver face image enhanced by the proposed method.

Figure 6. Comparison of image enhancement effects in different methods.

Then, the MSRCR image enhancement method mentioned in this paper is verified. The existing unenhanced automobile driver's face image is enhanced with the current method and the method of this paper. The results of the experiment are shown in Figure 6.

Finally, the automobile driver is tested under the single sample condition, and the size of the comfort value $P(x)$ of the face mentioned in Formula (17) is calculated by different methods. The results are compared with the actual value according to the calculated results. The comparison results are shown in Figure 7.

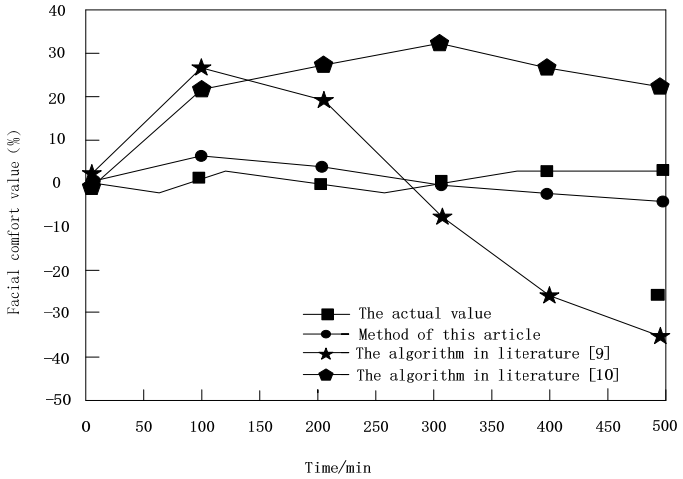

Figure 7. Comparison of comfort values in different methods.

As can be seen from Figure 7, the face comfort value $P(x)$ obtained by the method proposed in this paper is always close to the actual value, while the face comfort value $P(x)$ obtained by the method proposed by Lu et al. [7] and Geng et al. [8] has a larger deviation from the actual value, and the amplitude of the fluctuation is also large. It is proved that the proposed method has high detection accuracy, and the overall effect of fatigue detection is good.

4. Discussion

In this paper, the fatigue detection of the automobile driver is completed by the judgment of the human eye state. Therefore, we need to carry out the human eye feature extraction so as to facilitate the further fatigue identification of the driver. Before feature extraction, the size of three groups of eye images is set to 86 × 18, 90 × 18, and 96 × 18, so that the size of the picture is different and the dimensions of the feature vectors are different, which will not cause trouble with data processing. For the experimental process, the feature dimensions of eye image extraction are shown in Table 1.

Table 1. Eigenvector dimension.

	Pre-Processing Size	Post-Processing Size	Extraction Dimension
Group 1	86 × 18	45 × 10	450
Group 2	90 × 18	47 × 10	470
Group 3	96 × 18	50 × 10	500

The extracted feature vectors are used to judge the fatigue state of human eyes. In each group of 40 images, 10 positive samples and 10 negative samples were taken as the sequence set, and the remaining 20 images were taken as the test set. The accuracy evaluation method is obtained.

$$N\left(u_k, \sum\nolimits_k\right) = p(\omega_k) - \nabla_x \tag{20}$$

By comparing the accuracy with the traditional method, the fatigue test results are shown in Table 2.

Table 2. Fatigue testing accuracy (%) of different methods.

Detection Accuracy/%	Traditional Method	The Proposed Method
Group 1	80	96
Group 2	80	96
Group 3	65	86

According to Tables 2 and 3, the fatigue detection accuracy of this method is 16% higher than that of the traditional method. In terms of detection time, the fatigue detection time of this method is always lower than that of traditional methods. This method has obvious advantages in detection accuracy and detection time, and it can extract useful information.

Table 3. Fatigue detection time(s) of different methods.

Detection Time/s	Traditional Method	The Proposed Method
Group 1	60	5
Group 2	50	3
Group 3	48	1

5. Conclusions

This paper has completed the expected goal, and it has made great progress in the fatigue detection of the automobile driver, including the complex application environment or the large random noise, but these methods are still not ideal. There are still many problems to be studied in depth. The following aspects are improved and perfected:

(1) The proposed method adopted by each step in the study of text is carried out in different environments, and all of them can be integrated together to become a complete system, which is convenient to operate and improve the efficiency of operation.
(2) In this paper, some methods should be based on the change of fatigue detection in real time, following the changing trend of the fatigue testing environment and external interference, which can improve the fatigue testing process as much as possible and obtain the ideal fatigue test results.
(3) Due to the limited time, the problem of model checking under single sample condition has not been further studied. The overall computation time is long and has not yet reached the standard of large geometric models.

The above aspects will be discussed and studied in the future, looking forward to the application of the method to color cameras in the future, and I believe that satisfactory results will be achieved and contribute to the research and development in this field.

Author Contributions: C.X. did a linear simulation analysis. L.H. studied image effects and enhanced them. S.C. did fatigue tests. All authors conducted the experiments and analysed the results. All authors discussed the results and wrote the manuscript. All authors have read and agreed to the published version of the manuscript.

Funding: The research is supported by: National Key Research and Development Project (No. 2016YFC0501103); National Natural Science Foundation of China (No. 51804298); National Natural Science Foundation of China (No. 51774271); National Natural Science Foundation of China (No. 51674245).

Institutional Review Board Statement: Not applicable.

Informed Consent Statement: Not applicable.

Data Availability Statement: The data used to support the findings of this study are available from the corresponding author upon request.

Conflicts of Interest: The authors declare no conflict of interest.

References

1. Tayibnapis, I.R.; Koo, D.; Choi, M.; Kwon, S. A novel driver fatigue monitoring using optical imaging of face on safe driving system. In Proceedings of the International Conference on Control, Electronics, Renewable Energy and Communications, Bandung, Indonesia, 13–15 September 2016; IEEE: Toulouse, France, 2016; pp. 115–120.
2. Ilakiyaselvan, N.; Abraham, J.V.T.; Muralidhar, A.; Reddy, K.V. Real-time driver fatigue or drowsiness detection system using face image stream. *Int. J. Civ. Eng. Technol.* **2017**, *8*, 793–802.
3. Wang, D.; Wang, F.; Chen, X.; Yang, B. An improved image-based iris-tracking for driver fatigue detection system. In Proceedings of the 2017 36th Chinese Control Conference, Dalian, China, 26–28 July 2017; IEEE: Toulouse, France, 2017; pp. 11521–11526.
4. Ding, C.; Bao, T.; Karmoshi, S.; Zhu, M. Single sample per person facial image recognition with KPCANet and a weighted voting scheme. *Signal Image Video Process.* **2017**, *11*, 1213–1220. [CrossRef]
5. Azarudheen, S.; Pradeepaveerakumari, K. Determination of skip lot sampling plan with single sampling plan as reference plan under the conditions of intervened poisson distribution. *J. Stat. Manag. Syst.* **2016**, *19*, 771–780. [CrossRef]
6. Fu, R.; Wang, H.; Zhao, W. Dynamic driver fatigue detection using hidden Markov model in real driving condition. *Expert Syst. Appl.* **2016**, *63*, 397–411. [CrossRef]
7. Lu, W.; Hu, H.Y.; Wang, J.P.; Wang, L.; Deng, Y.M. Automobile driver fatigue detection based on convolutional neural network facial image recognition. *J. Agric. Eng.* **2018**, *34*, 192–199.
8. Geng, L.; Yuan, F.; Xiao, Z.T. Driver fatigue detection method based on facial behavior analysis. *Comput. Eng.* **2018**, *44*, 274–279.
9. Cai, J.; Chen, J.; Liang, X. Face to face change dictionary learning single sample facial image recognition. *Minitype Microcomput. Syst.* **2015**, *36*, 2079–2083.
10. Li, Z.J.; Chen, L.K.; Peng, J.; Wu, Y. Automatic detection of driver fatigue using driving operation information for transportation safety. *Sensors* **2017**, *17*, 1212. [CrossRef] [PubMed]
11. Li, Z.; Sun, G.; Zhang, F.; Jia, L.; Zheng, K.; Zhao, D. Smartphone-based fatigue detection system using progressive locating method. *IET Intell. Transp. Syst.* **2016**, *10*, 148–156. [CrossRef]
12. Zhao, L.; Wang, Z.; Wang, X.; Liu, Q. Driver drowsiness detection using facial dynamic fusion information and a DBN. *IET Intell. Transp. Syst.* **2018**, *12*, 127–133. [CrossRef]
13. Sun, X.; Pan, T.; Ren, F. Facial expression recognition based on ROI-KNN convolution neural network. *J. Autom.* **2016**, *42*, 883–891.
14. Hu, J.; Zheng, B.; Wang, C.; Zhao, C.; Hou, X.; Pan, Q.; Xu, Z. A survey on multi-sensor fusion based obstacle detection for intelligent ground vehicles in off-road environments. *Front. Inf. Technol. Electron. Eng.* **2020**, *21*, 675–692. [CrossRef]
15. Jia, X.Y.; Zhou, L.Y.; Ren, J.; Zhang, N. Research on face fatigue detection method based on facial feature fusion. *Power Grid Clean Energy* **2016**, *32*, 17–21.
16. Garcia-Planas, M.I.; Klymchuk, T. Perturbation analysis of a matrix differential equation X = ABx. *Appl. Math. Nonlinear Sci.* **2018**, *3*, 97–104. [CrossRef]
17. Durur, H.; Kurt, A.; Tasbozan, O. New travelling wave solutions for KdV6 equation using sub equation method. *Appl. Math. Nonlinear Sci.* **2020**, *5*, 455–460. [CrossRef]
18. Ji, X.S.; Wang, R.F. Facial expression recognition using adaptive weighted LGCP and fast sparse representation. *Comput. Eng. Appl.* **2017**, *53*, 158–162.
19. Niu, G.T.; Wang, C.M.; Meng, H.B. Facial fatigue recognition based on multi-scale sparse representation. *Comput. Sci.* **2016**, *43*, 282–285.
20. Jiang, Q.; Shao, F.; Gao, W.; Chen, Z.; Jiang, G.; Ho, Y.-S. Unified no-reference quality assessment of singly and multiply distorted stereoscopic images. *IEEE Trans. Image Process.* **2019**, *28*, 1866–1881. [CrossRef] [PubMed]
21. Zenggang, X.; Zhiwen, T.; Xiaowen, C.; Xue-Min, Z.; Kaibin, Z.; Conghuan, Y. Research on image retrieval algorithm based on combination of color and shape features. *J. Signal Process. Syst.* **2021**, *93*, 139–146. [CrossRef]
22. He, J.; Fang, L.-Z.; Cai, J.-F.; He, Z.-W. Fatigue driving detection based on ASM and skin color model. *Comput. Eng. Sci.* **2016**, *38*, 1447–1453.